

Classification of unlabeled observations in Species Distribution Modelling using Point Process Models.

Emy Guilbault¹, Ian Renner¹, Michael Mahony², Eric Beh¹.

Emy.Guilbault@uon.edu.au

April 16, 2019

¹ *School of Mathematical and Physical Sciences, University of Newcastle, Callaghan, NSW, Australia.*

² *School of Environmental and Life Sciences, University of Newcastle, Callaghan, NSW, Australia.*

1 Abstract

1. *Species distribution modelling, which allows users to predict the spatial distribution of species with the use of environmental covariates, has become increasingly popular, with many software platforms providing tools to fit species distribution models. However, the species observations used in species distribution models can have varying levels of quality and can have incomplete information, such as uncertain species identity.*

2. *In this paper, we develop two algorithms to reclassify observations with unknown species identities which simultaneously predict different species distributions using spatial point processes. We compare the performance of the different algorithms using different initializations and parameters with models fitted using only the observations with known species identity through simulations.*

3. *We show that performance varies with differences in correlation among species distributions, species abundance, and the proportion of observations with unknown species identities. Additionally, some of the methods developed here outperformed the models that didn't use the misspecified data.*

4. *These models represent a helpful and promising tool for opportunistic surveys where misidentification happens or for the distribution of species newly separated in their taxonomy.*

Keywords: Presence-only data - Ecological statistics - Misidentification - Classification - Mixture modelling - EM algorithm - Machine learning

2 Introduction and background

Species distribution modelling has been a popular topic in ecological statistics over the past decade. Many tools and methods have been developed to provide a means to explore the distributions of species

29 Inoue *et al.*, 2017; Schank *et al.*, 2017). Although there are a large number of algorithms and software
30 platforms that can fit species distribution models (SDMs), generalization of these methods and specific
31 applications to real data sets can be tricky (Burnham & Anderson, 2002; Aarts *et al.*, 2012; Guillera-Aroita
32 *et al.*, 2015).
33

34 The most common sources of species information used in SDMs are presence-only (PO) and presence-
35 absence (PA) data. PO data only contains information about species presence, in contrast to PA data
36 which records both where species have been found present and where they have not been found (Warton
37 & Shepherd, 2010; Renner *et al.*, 2015). Although PA data is generally of higher quality, it is also less
38 common than PO data because it requires more rigorous planning to visit a set of pre-determined sites.
39 On the other hand, PO data sets are very common, arising from surveys or opportunistic sightings, but
40 they usually have lower quality (van Strien *et al.*, 2013; Ruete & Leynaud, 2015). Point process models
41 (PPMs) are a common tool for fitting SDMs to analyze PO data (Warton & Shepherd, 2010; Mi *et al.*,
42 2014; Renner *et al.*, 2015) and have been used to fit models for real datasets and simulated data (Baddeley
43 *et al.*, 2006; Illian *et al.*, 2012; Renner & Warton, 2013; Baddeley *et al.*, 2015).
44

45 Unreliable or unknown species observation identification is also a main concern in ecology. For example,
46 species records can become confounded when species taxonomy changes (Mahony *et al.*, 2006). Conservation
47 planning efforts depend on clear identification of species and understanding of their distributions and
48 habitat requirements (Franklin, 2013; Guisan *et al.*, 2013). Such concerns are very rarely considered while
49 building SDMs, as people usually clean the data or make some assumptions to avoid such identification
50 problems.

51 Mixture modelling is a common tool used to represent complex distributions and aims to identify
52 different groups within a dataset while modelling heterogeneity (Martinez, 2015). In communities or
53 groups of individuals/species it is possible to classify or cluster them according to covariate information
54 by using finite mixture modelling (McLachlan & Peel, 2000; Frame & Jammalamadaka, 2007; Dunstan
55 *et al.*, 2013; Fernández-Michelli *et al.*, 2016). One particular application of this approach is to deal with
56 over-dispersed data and to model the different ecological processes at the same time for a single species or
57 for different species in order to classify them (Matthews *et al.*, 2001; Zhang *et al.*, 2004; Tracey *et al.*,
2013).

58 Machine learning algorithms are also becoming more common in statistical ecology because they can
59 deal with unknown information and recognize some structure in the data (Hastie *et al.*, 2001; Thessen, 2016;
60 Browning *et al.*, 2018). Some algorithms can group observations with similar characteristics (unsupervised
61 learning) and some use separate labeled datasets (supervised learning) or partially labeled data within the
62 studied dataset (semi-supervised learning) to classify the observations (Wendel *et al.*, 2015; Fernández-

63 algorithms to fit PPMs in a Bayesian framework (Tran, 2017; Vo *et al.*, 2018), but the literature on using
64 machine learning algorithms to fit PPMs is not yet well-developed. Additionally, several R packages have
65 been developed to deal with machine learning procedures (Benaglia *et al.*, 2009; Iovleff, 2018), but none
66 accommodate the intersection of point process modelling with mixture modelling or machine learning
67 algorithms.
68

69 In this paper we develop new tools for fitting models to multi-species PO data with partial species
70 identification by combining the PPM framework with mixture modelling and machine learning approaches
71 to accommodate incomplete labelling. These tools implement two algorithms to reclassify the unreliable
72 observations to belong to one of the existing species. The first tool fits mixtures of PPMs to all available
73 data with an Expectation-Maximization (EM) algorithm and uses them to classify the unreliable points.
74 This method will be called *Mixture method*. The second tool employs an iterative technique to fit
75 separate PPMs to points with known labels augmented by some points with unknown labels depending
76 on classification probabilities at each iteration. This method will be hereafter known as the *Loop method*.
77 Using simulations, we compare the performance in classification and prediction for the proposed algorithms
78 to the simple, standard approach of fitting individual PPMs to the points with known species labels only.
79 We found that performance varied based on the choice of initialization and algorithm parameters but
80 some of the methods can outperform the fitting of individual PPMs.

81 **3 New modelling methods**

82 **3.1 Notation**

83 The fitted point process models in our proposed methods make use of a total of $M + N + Q$ locations as
84 follows:

85 Let $\mathbf{s}_1 = \{s_1, \dots, s_{m_1}\}$, $\mathbf{s}_2 = \{s_{m_1+1}, \dots, s_{m_1+m_2}\}$, \dots , $\mathbf{s}_K = \{s_{M-m_K+1}, \dots, s_M\}$ be vectors that
86 contain all of the observed locations with known species identities $1, 2, \dots, K$, respectively. These are
87 represented by the orange, purple, and turquoise dots in Figure 1 for a hypothetical dataset. Let
88 $|\mathbf{s}_1| = m_1, |\mathbf{s}_2| = m_2, \dots, |\mathbf{s}_K| = m_K$ be the number of observed locations with known species identity
89 for each of the K species. We collect the $M = m_1 + m_2 + \dots + m_K$ total locations with known species
90 identities of all K species in $\mathbf{s} = \{\mathbf{s}_1, \mathbf{s}_2, \dots, \mathbf{s}_K\}$. Let $\mathbf{u} = \{s_{M+1}, \dots, s_{M+N}\}$ contain the N observed
91 locations with uncertain species identities. These are represented by the black question marks in Figure 1.
92 Let $\mathbf{q} = \{s_{M+N+1}, \dots, s_{M+N+Q}\}$ contain the locations of Q quadrature points placed along a regular
93 $c_1 \times c_2$ grid throughout the study region (Figure 1). Each quadrature point is placed at the center of one
94 of Q unique rectangular grid cells throughout the study region. Let $c(s)$ be the grid cell in which location

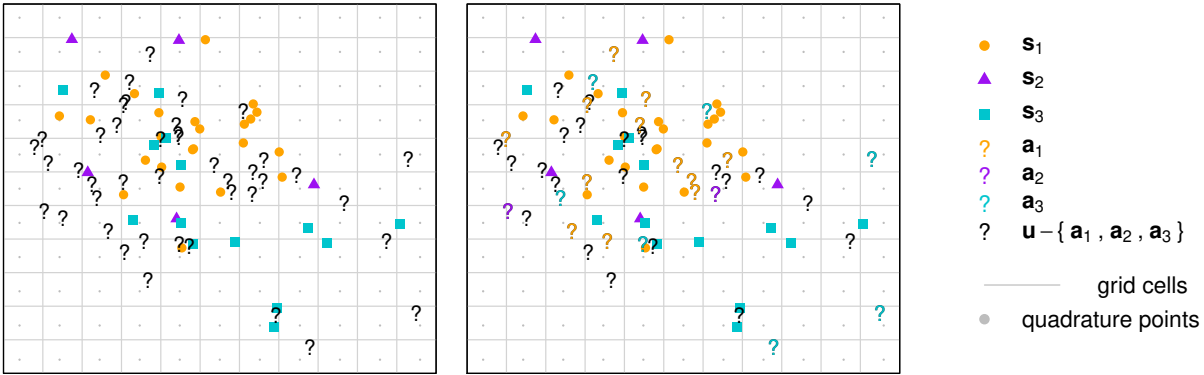


Figure 1: Three illustrative point patterns. The orange, purple, and turquoise colored dots represent locations with known species identity, \mathbf{s}_1 , \mathbf{s}_2 , and \mathbf{s}_3 . The gray dots represent quadrature points \mathbf{q} , which are spaced evenly along a regular grid such that one quadrature point is at the centre of each rectangular grid cell. The black question marks (left) represent observed locations \mathbf{u} with uncertain species identity. The locations in $\mathbf{a}_1 \in \mathbf{u}$, $\mathbf{a}_2 \in \mathbf{u}$, and $\mathbf{a}_3 \in \mathbf{u}$ which are reclassified as belonging to one of the species are represented by coloured question marks (right).

96 3.2 Loop methods

97 The three loop algorithms proceed by iterating between steps that augment the vectors of locations with
 98 known species identities $\mathbf{s}_1, \mathbf{s}_2, \dots, \mathbf{s}_K$ with locations $\mathbf{a}_1 \subset \mathbf{u}, \mathbf{a}_2 \subset \mathbf{u}, \dots, \mathbf{a}_K \subset \mathbf{u}$, update the quadrature
 99 weights, and fit point process models as follows:

- 100 1. Fit K initial point process models using the vectors of observed locations with known species identity
 101 $\mathbf{s}_1, \mathbf{s}_2, \dots, \mathbf{s}_K$.
- 102 2. Compute the predicted intensities $\hat{\mu}_i(s)$ for all $s \in \{\mathbf{s} \cup \mathbf{u}\}$ for $i \in \{1, \dots, K\}$.
3. Derive an $(M + N) \times K$ matrix of membership probabilities ω , where

$$\omega = \begin{bmatrix} \omega_1(s_1) & \omega_2(s_1) & \dots & \omega_K(s_1) \\ \omega_1(s_2) & \omega_2(s_2) & \dots & \omega_K(s_2) \\ \vdots & \vdots & \dots & \vdots \\ \omega_1(s_{M+N}) & \omega_2(s_{M+N}) & \dots & \omega_K(s_{M+N}) \end{bmatrix}$$

103 The membership probability of location s for species i is defined as

$$\omega_i(s) = \begin{cases} \mathbb{1}(s \in \mathbf{s}_i) & : s \in \mathbf{s} \\ \frac{\hat{\mu}_i(s)}{\sum_{j=1}^K \hat{\mu}_j(s)} & : s \in \mathbf{u}. \end{cases} \quad (1)$$

104 That is, the membership probabilities for the locations with known species identity are 1 for the
 105 correct species and 0 otherwise, and for the locations with unknown species identity, they are

107 4. Define an augmented vector for species i as $\mathbf{y}_i = \mathbf{s}_i \cup \mathbf{a}_i$ for all $i \in \{1, \dots, K\}$. We define \mathbf{a}_i as
 108 follows:

- 109 • For the **Normal** method, $\mathbf{a}_i = \mathbf{u}$ (left panel of Figure 2).
- 110 • For the **Loop grW** method, $\mathbf{a}_i = \mathbf{u}_{[\omega_i(s) \geq \delta]}$, where δ is a minimum membership proba-
 111 bility threshold that takes the following values successively at each iteration $\{\delta_{\max}, \delta_{\max} -$
 112 $\delta_{\text{step}}, \dots, \delta_{\min}\}$. That is, the Loop grW method augments the locations with known species
 113 identity i with the locations with unknown species identity with membership probabilities for
 114 species i that are higher than the current threshold δ (middle panel of Figure 2).
- 115 • For the **Loop hgW** method, $\mathbf{a}_i = \mathbf{u}_{[\omega_i(s) \geq \omega_{i,(M+N-a+1)}]}$, where $\omega_{i,(j)}$ represents the j^{th} smallest
 116 entry of vector $\boldsymbol{\omega}_i$, the i^{th} column of $\boldsymbol{\omega}$, and a represents the number of locations to be augmented.
 117 We set a to be the same integer for all K species for some a between 1 and $\lfloor \frac{N}{K} \rfloor$ then at each
 118 iteration a is increased by one (right panel of Figure 2).

119 5. Update the quadrature weights for each species. First, assign each location in $\{\mathbf{y}_1, \dots, \mathbf{y}_K, \mathbf{q}\}$ to a
 120 grid cell. Then, compute the vector of quadrature weights \mathbf{w}_i for all points $t \in \{\mathbf{y}_i \cup \mathbf{q}\}$ as follows:

$$w_i(t) = \frac{c_1 \times c_2 \times \omega_i(t)}{1 + \sum_{s \in \{\mathbf{y}_i \cup \mathbf{q}\}} \mathbb{1}(c(s) = c(t)) \omega_i(s)}. \quad (2)$$

121 This way of computing quadrature weights is an extension of standard quadrature weight schemes
 122 for point process models (Berman & Turner, 1992), in which the weight for location s is equal to the
 123 area of the grid cell $c(s)$ that contains s divided by the total number of quadrature and observed
 124 locations in $c(s)$. Here, we divide the area of the grid cell by the sum of the membership probabilities
 125 of the observed locations in the grid cell (both with and without known species identities) plus 1
 126 (for the one quadrature point in the grid cell).

127 6. Fit point process models using the augmented vector \mathbf{y}_i , quadrature points \mathbf{q} and quadrature weights
 128 \mathbf{w}_i for all species $i \in \{1, \dots, K\}$.

129 7. Return to step 2 and stop when we either reach likelihood convergence or we reach a maximum
 130 number of iterations that is different depending on the method chosen. Likelihood convergence is
 131 determined by:

$$\delta_l = \frac{\sum_{j=1}^K \left| \ell_{h+1}^j(\boldsymbol{\beta}) - \ell_h^j(\boldsymbol{\beta}) \right|}{\left(\sum_{j=1}^K \ell_h^j(\boldsymbol{\beta}) \right)} < \epsilon \quad (3)$$

132 for some choice of ϵ , where $\ell(\boldsymbol{\beta})_h^j$ is the fitted log-likelihood for the j^{th} species at the h^{th} iteration.

133 The maximum number of iterations varies for the different methods, as follows:

135
136
137
138
139
140
141

- For the **Normal** method, the maximum number of iterations is set by the user. We set the default number of iterations to be 50.
- For the **Loop grW** method, the maximum number of iterations is determined by the choice of δ_{\max} , δ_{step} , and δ_{\min} .
- For the **Loop hgW** method, the maximum number of iterations is $\lfloor \frac{N}{K} \rfloor - a_1$, where $\lfloor c \rfloor$ rounds the number c down to the nearest integer, and a_1 is the first value of a chosen by the user. In the case of decimals numbers, only the floor is considered as the we can't add more points than available per species.

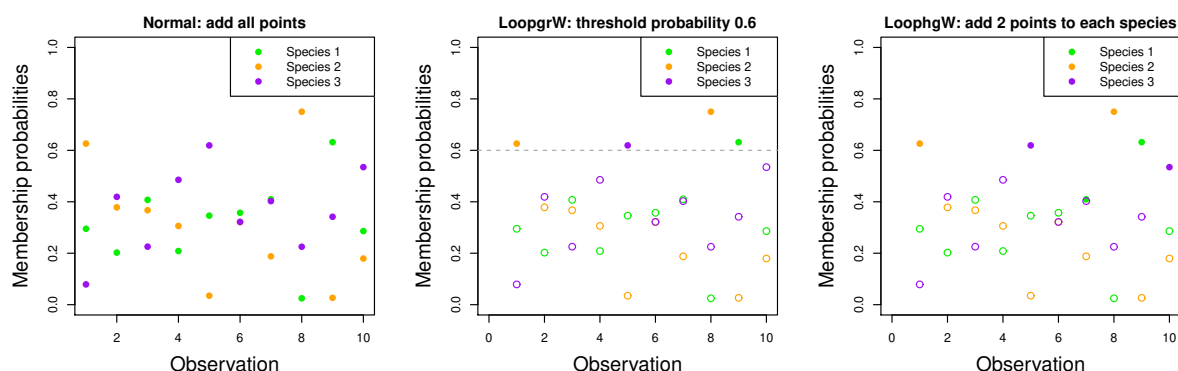


Figure 2: (Left) Normal Loop function. We add all points with unknown species labels to each species, using membership weights that are proportional to the fitted intensities. (Middle) Method Loop grW function. We add all points with membership probabilities greater than a threshold δ_{\max} , then we decreases from that value to a minimum of δ_{\min} by increments of δ_{step} . (Right) Method Loop hgW function. We add the a points with highest membership probabilities to each species, increasing the number a from 1 to $\lfloor \frac{N}{K} \rfloor$.

142 3.3 Mixture of PPMs method

143 The four mixture algorithms can be fitted by maximizing a log-likelihood function and reclassifying the
144 locations with uncertain identity using an EM algorithm framework. The algorithm proceeds as follows:

1. We initialize the membership probabilities ω for each location s for each species i in one of the
146 following ways:
 - 147 • For the **knn method**, we calculate the distance $d_i(s)$ of each location s to the k^{th} nearest
148 neighbor of species i , for all K species. We calculate the membership probability of location s
149 for species i using:

$$\omega_i(s) = \begin{cases} \mathbb{1}(s \in \mathbf{s}_i) & : s \in \mathbf{s} \\ \frac{z_i(s)}{\sum_{j=1}^K z_j(s)} & : s \in \mathbf{u}. \end{cases} \quad (4)$$

$$z_i(s) = \frac{\min_{1 \leq j \leq K} d_j(s)}{d_i(s)} \quad (5)$$

- 151 • For the **kmeans method**, we define $\omega_i(s)$ as in (4) but define $z_i(s)$ as

$$z_i(s) = \frac{\min_{1 \leq j \leq K} d_j^C(s)}{d_i^C(s)}, \quad (6)$$

152 where $d_i^C(s)$ is the distance to the i^{th} centroid of the i^{th} cluster.

- 153 • For the **random method**, we define $\omega_i(s)$ as in (4) and $z_i(s)$ is drawn randomly from a
154 uniform distribution:

$$z_i(s) \sim U[0, 1] \quad (7)$$

- 155 • For the **equal method**, we assign equal membership probabilities for the locations with
156 uncertain identity:

$$\omega_i(s) = \begin{cases} \mathbb{1}(s \in \mathbf{s}_i) & : s \in \mathbf{s} \\ \frac{1}{K} & : s \in \mathbf{u}. \end{cases} \quad (8)$$

157 Regardless of the initialization method, the sum of membership probabilities across the all species is
158 equal to 1 for all points.

- 159 2. Classify the locations in \mathbf{u} to belong to one of the K species based on the membership probabilities
160 ω .

- 161 3. Fit a point process model using a marked point pattern, where each observation s has a mark defined
162 by the known or classified identity among the K species.

- 163 4. Compute the predicted intensities $\hat{\mu}_i(s)$ for all $s \in \{\mathbf{s} \cup \mathbf{u}\}$ for $i \in \{1, \dots, K\}$.

- 164 5. E step: We first get the predicted values of each species at the locations $s \in \{\mathbf{s} \cup \mathbf{u}\}$ and calculate
165 the predicted intensity of the mixture of K densities using:

$$f(s) = \sum_{i=1}^K \pi_i \times f_i(s), \quad (9)$$

166 where $f_i(s)$ is the density at location s for the i^{th} component and π_i is the mixing proportion or
167 weight of the i^{th} species in the mixture.

- 168 6. We calculate new membership probabilities for each unknown point of \mathbf{u} using:

$$\omega_i(s) = \frac{\hat{\mu}_i(s)}{\sum_{i=1}^k \hat{\mu}_i(s)}, \quad (10)$$

169 labels, the membership probabilities are set to 1 for the correct species label and 0 otherwise.

171 7. M step: Classify the locations in \mathbf{u} to belong to one of the K species. The classification for each
172 point s corresponds to the highest membership probability $\omega_i(s)$ for $i \in \{1, \dots, K\}$. We compute
173 each species' proportion of the whole by summing the membership probabilities for each species
174 across both \mathbf{s} and \mathbf{u} .

175 8. Compute a marked PPM based on the updated classifications and membership probabilities.

176 9. Calculate the model log likelihood using:

$$\ell(\boldsymbol{\beta}) = \sum_{s \in \mathbf{s} \cup \mathbf{u}} f(s, \boldsymbol{\beta}) = \sum_{s \in \mathbf{s} \cup \mathbf{u}} \log \sum_{i=1}^K \pi_i \times f(s, \beta_i) \quad (11)$$

177 10. Repeat steps 4-9 until we achieve likelihood convergence, defined as follows:

$$\frac{|\ell_{h+1}(\boldsymbol{\beta}) - \ell_h(\boldsymbol{\beta})|}{(1 + |\ell_{h+1}(\boldsymbol{\beta})|)} < \epsilon \quad (12)$$

178 where $\ell_h(\boldsymbol{\beta})$ is the log-likelihood at the h^{th} iteration and ϵ is a pre-specified tolerance level.

179 4 Simulation framework

180 4.1 Simulation data

181 To compare the performance of the different algorithms, we simulated patterns \mathbf{t}_1 , \mathbf{t}_2 , and \mathbf{t}_3 of individuals
182 for three species based on “true” distributions defined by four different predictors. Because performance
183 could varied based on sample size, the correlations $\rho_{i,j}$ among the species distributions, and the proportion
184 of observations with unknown labels, we consider similar and different low abundances by randomly
185 simulating numbers of points between 20 and 50 for the species as well as the correlation between the true
186 species distributions:

- 187 • Case 1: at least two species i and j have distributions that are highly correlated ($|\rho_{i,j}| \geq 0.85$ for
188 some $i, j \in \{1, 2, 3\}$)
- 189 • Case 2: no two species have highly correlated distributions ($|\rho_{i,j}| < 0.45$ for all $i, j \in \{1, 2, 3\}$)

190 We chose these values for abundances as they would be small enough such that potential value of adding
191 points with unknown species identities could be investigated, and we chose these cutoffs for correlation to
192 create clearly distinguishable contexts.

193 We then created locations with unknown labels \mathbf{u} by hiding uniformly at random a certain proportion of
194 the total observations (20%, 50% and 80%). The locations in \mathbf{t}_1 , \mathbf{t}_2 , and \mathbf{t}_3 that retained their true species

196 Simulations were conducted using the version 3.4.2 of R (R Core Team, 2017) and used high performance
197 computing to implement 1000 simulations each for different combinations of abundances, correlation
198 among species distributions, and proportions of observations with unknown labels. We also tested different
199 parameters for the knn initialization of the mixture algorithm (the value of k neighbors), the Loop grW
200 function (the maximum threshold δ_{\max} , minimum threshold δ_{\min} and the step size δ_{step}) and the Loop
201 hgW function (initial number of points added to the point pattern a).

202 4.2 Suite of Evaluation tools

203 We consider various measures of performance for comparing the distributions. For classification methods,
204 misclassification/accuracy analysis is a common measure of performance (Wendel *et al.*, 2015). We choose
205 the highest mixing weight for each observation to determine the labeling when computing accuracy. We
206 also compared the final membership probabilities of the correct labels of each point to 1 (the true weight)
207 with a residual sum of squares (RSS).

$$\text{RSS} = \sum_{i=1}^K \sum_{s \in \mathbf{t}_i} (\omega_i(s) - 1)^2, \quad (13)$$

208 where $\omega_i(s)$ is the final membership probability for location s for the correct species i computed using
209 the methods outlined in sections 3.2 and 3.3. Considering residual sum of squares (RSS) alone does not
210 provide a reliable comparison because the number of unknown observations can vary, so we consider
211 meanRSS instead to standardize the measure for all fitted models:

$$\text{meanRSS} = \frac{\text{RSS}}{N}, \quad (14)$$

212 where N is the number of observations with uncertain species identities.

213 We also considered measures that compare the true distribution from which we generate the points to
214 the predicted distributions of the model. We use a sum of correlations between the true and predicted
215 distributions across all species (hereafter referred to as ‘sumcor’) to assess how well the predicted
216 distributions align with the true distributions. We can use various correlation measures such as Pearson’s
217 correlation coefficient, Kendall’s τ or Spearman’s ρ when computing sumcor.

218 Another global measure of predictive performance of the intensity estimates is the Integrated Mean Square
219 Error (IMSE) (Swanepoel, 1988; Es, 1997). The function is defined as:

$$\text{IMSE} = E \left(\int_{-\infty}^{+\infty} ((\hat{f}_n(x) - f(x))^2) dx \right), \quad (15)$$

221 intensities to be able to compare each methods even if different number of points are considered and
222 compute the IMSE using the values of the true and predicted intensities at the quadrature points \mathbf{q} , and
223 sum across the 3 species.

224 5 Results

225 Here we present the results of the simulations, with more detailed results appearing in the Appendix.
226 In this section, we only present the results from the knn, Lopp grW, Loop hgW and individual PPM
227 methods that displayed the best performances. First, we present the model performances from varying
228 data parameters (abundance, correlation and percentage of hidden labeled data). The individual PPM
229 results will be used as a point of comparison with the other methods as the individual method does
230 not include any of the points with unknown labels. We, then, focus on varying model parameters in
231 the different methods (the value of k for knn, the values of δ_{\max} , δ_{\min} and δ_{step} for Loop grW and the
232 value of a for Loop hgW). For these results, we set $k = 1$, $\delta_{\max} = 0.5$, $\delta_{\min} = 0.1$, $\delta_{\text{step}} = 0.1$ and $a = 5$
233 according to the algorithm parameters tests presented in section 5.2. For the performance results, the
234 sumcor methods displayed the result using the Pearson correlation coefficient.

235 5.1 Varying species distributions

236 5.1.1 Different abundances and correlated distributions

237 In Figure 3, we consider different low abundances ($m_1 = 32$, $m_2 = 42$ and $m_3 = 23$) and where two
238 distributions are highly correlated. With regard to classification performance, the different modelling
239 methods have similar levels of accuracy, although when comparing meanRSS, the individual and Loop
240 grW methods seem to outperform the other methods, especially as we increase the proportion of hidden
241 observations. With regard to predictive performance, the Loop grW method appears to have the greatest
242 performance when measured by IMSE and sumcor, particularly for 50% and 80% of hidden observations.
243 The Loop hgW method performs comparably to the individual PPM method, although its performance
244 gets relatively better as we increase the proportion of hidden observations. The knn method has the
245 highest IMSE for 50% and 80% of hidden observations, but it is competitive with the individual PPM
246 and loop hgW method when comparing sumcor. See Tables 1 and 2 in the Appendix for a comparison of
247 means and medians across all of these measures.

248 When examining the predicted intensities with 80% of the observations with hidden species identities, the
249 true pattern appears best captured by the Loop grW method (Figure 4), consistent with sumcor. The
250 Loop hgW method tends to overpredict the intensities.

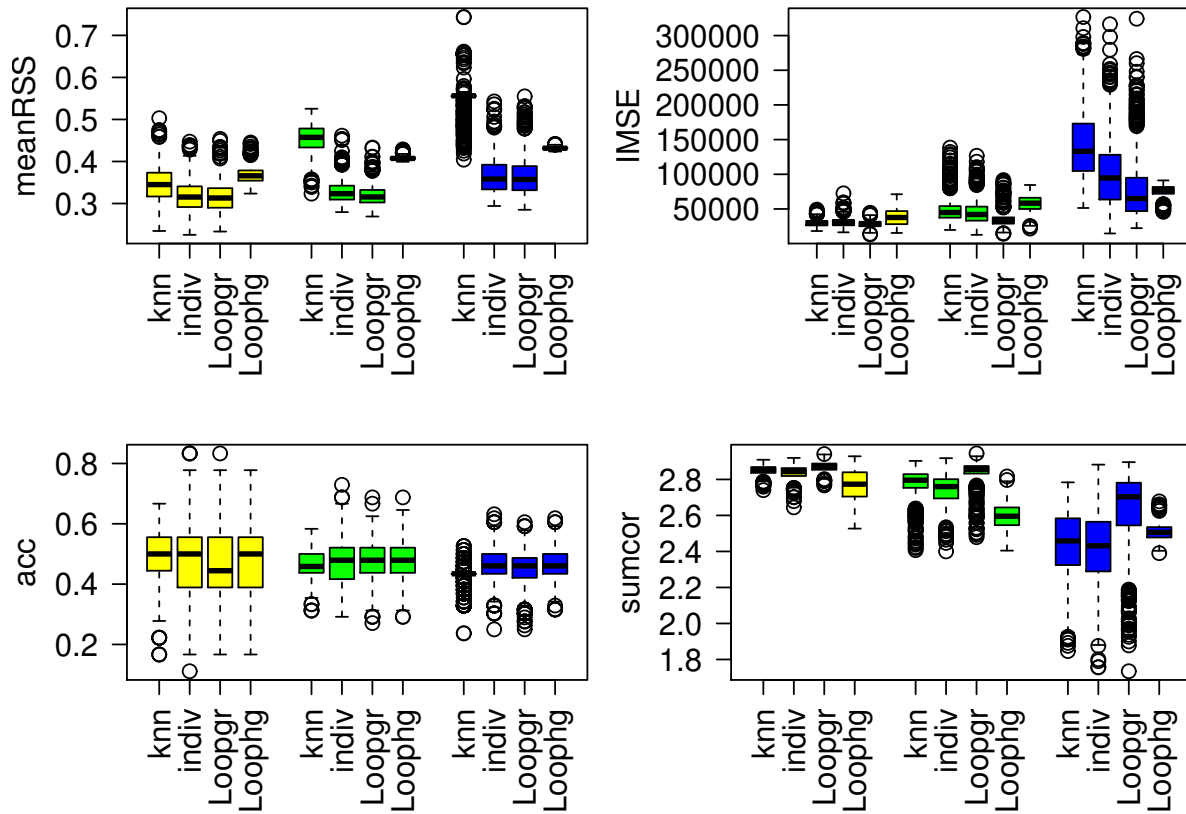


Figure 3: Measures of performance for the knn, individual, Loop grW and Loop hgW methods. Each color boxplot represents a different percentage of hidden observation: in yellow are the performances with 20% of hidden observations, in green with 50% and in blue with 80%. The parameters of abundances and correlation are: $m_1 = 32$, $m_2 = 42$, $m_3 = 23$; $\rho_{1,2} = 0.85$, $\rho_{1,3} = -0.09$, $\rho_{2,3} = 0.20$.

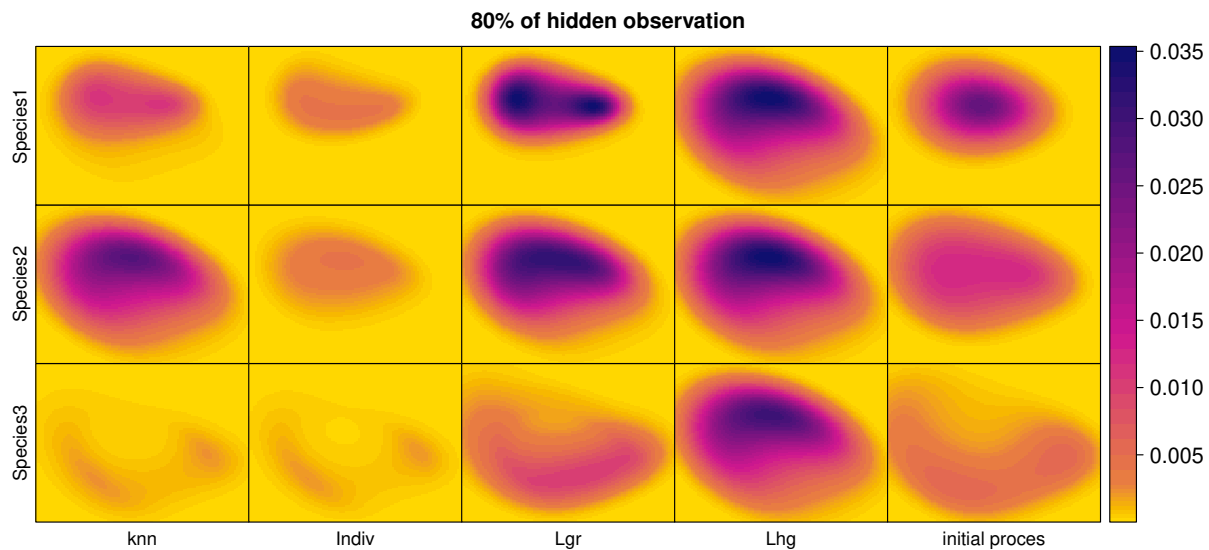


Figure 4: Predicted intensities obtained for the knn, individual, Loop grW and Loop grW methods and the initial intensities from the process with 80% of hidden observations. The parameters of abundances and correlation are: $m_1 = 32$, $m_2 = 42$, $m_3 = 23$; $\rho_{1,2} = 0.85$, $\rho_{1,3} = -0.09$, $\rho_{2,3} = 0.20$.

5.1.2 Similar abundances and correlated distributions

252 In Figure 5, we consider similar abundances ($m_1 = 33$, $m_2 = 34$ and $m_3 = 35$) and where two distributions
 253 are highly correlated. With regard to classification performance, the different modelling methods have
 254 similar levels of accuracy, except the knn method does relatively poorly with 80% of the observations
 255 hidden. The knn method also suffers worse performance as measured by meanRSS at 50% and 80% of
 256 hidden observations. Measures of predictive performance are similar to the case with different abundances
 257 and correlated distributions. The Loop grW method appears to outperform the others as the proportion
 258 of hidden observations increases, with the Loop hgW method competitive with the individual PPM
 259 method. The knn method appears to do worse with 80% hidden observations when measured by IMSE.
 260 See Tables ?? and ?? in the Appendix for comparisons of means and medians across all of these measures.
 261 With 80% hidden observations, the Loop Loop grW method appears to be best aligned with the true
 262 intensities, as shown in Figure 6.

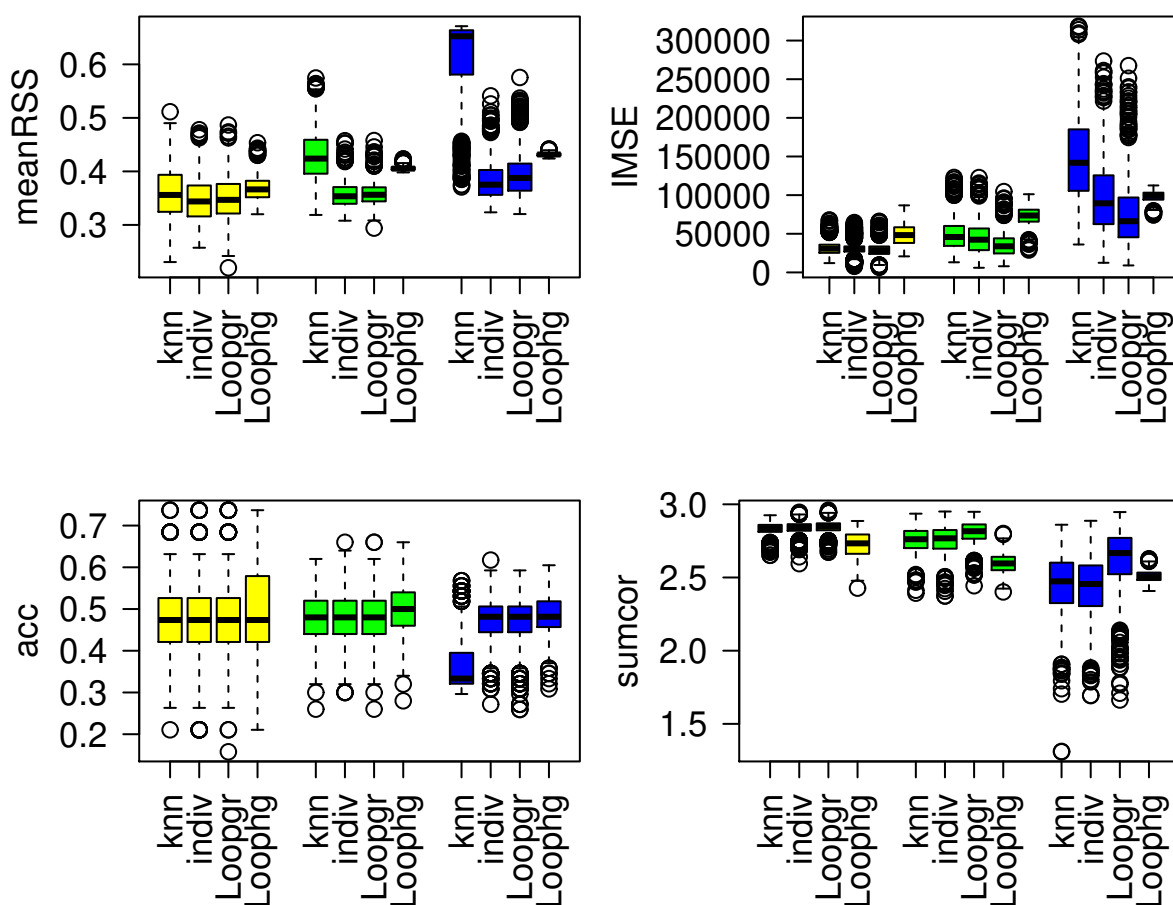


Figure 5: Measures of performance for the knn, individual, Loop grW and Loop hgW methods. Each color represents a different percentage of hidden observations: in yellow are the performances with 20% of hidden observations, in green with 50% and in blue with 80%. The parameters of abundances and correlation are: $m_1 = 33$, $m_2 = 34$, $m_3 = 35$; $\rho_{1,2} = 0.85$, $\rho_{1,3} = -0.09$, $\rho_{2,3} = 0.20$.

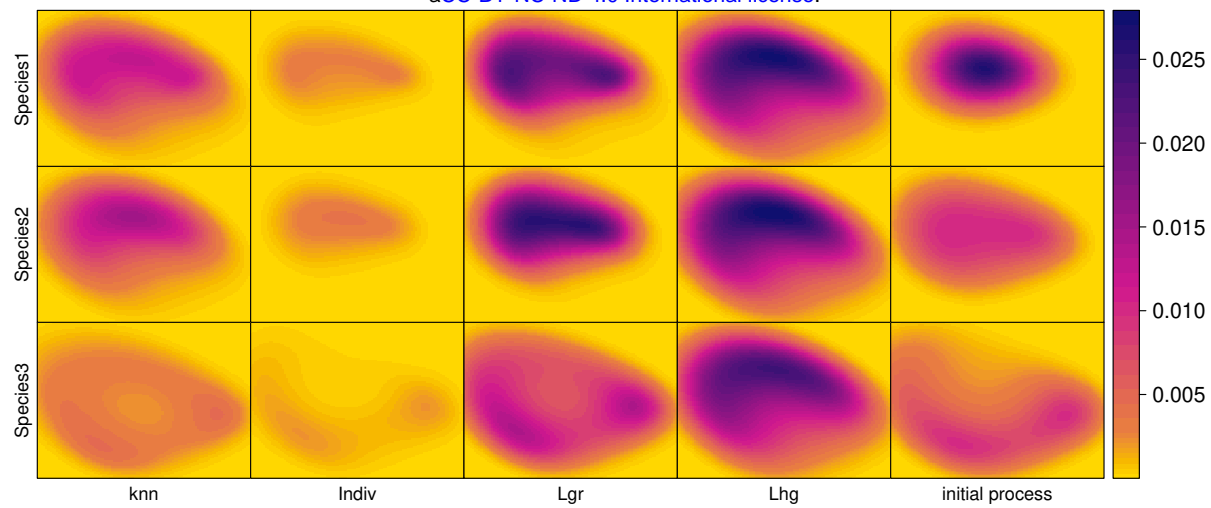


Figure 6: Predicted intensities obtained for the knn, individual, Loop grW and Loop hgW methods and the initial intensities from the process with 80% of hidden observations. The parameters of abundances and correlation are: $m_1 = 33$, $m_2 = 34$, $m_3 = 35$; $\rho_{1,2} = 0.85$, $\rho_{1,3} = -0.09$, $\rho_{2,3} = 0.20$.

263 5.1.3 Different abundances and non correlated distributions

264 In Figure 7, we consider different abundances ($m_1 = 42$, $m_2 = 31$ and $m_3 = 25$) and where none of
265 the distributions have high correlations. The classification performance and predictive performance
266 comparisons look similar to the case of similar abundances and correlated distributions as shown in
267 Figure 5, with the knn method having the worst classification performance described here at 50% and 80%
268 of hidden observations and the Loop grW method outperforming the others in predictive performance,
269 while the Loop hgW method is competitive with the individual PPM method and the knn method lags
270 behind with IMSE at 80% of hidden observations. Tables 5 and 6 in the Appendix contains the means
271 and medians across all performance measures for this context.

272 With 80% of hidden observation as shown in Figure 8, the Loop hgW method for species 1 and 3 and the
273 Loop grW method for species 2 and 3 are the closest to the initial process.

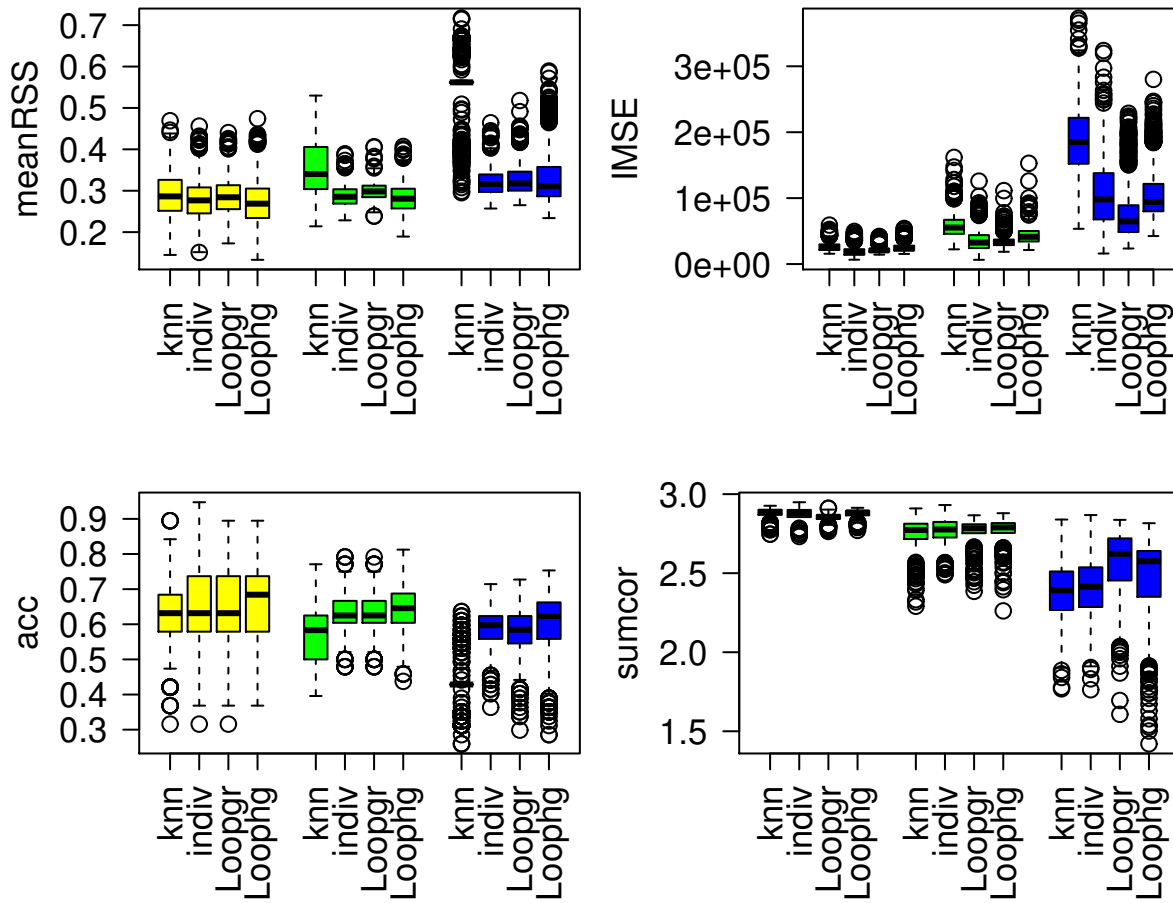


Figure 7: Measures of performance for the knn, individual, Loop grW and Loop hgW methods. Each color represents a different percentage of hidden observations: in yellow are the performances with 20% of hidden observations, in green with 50% and in blue with 80%. The parameters of abundances and correlation are: $m_1 = 42$, $m_2 = 31$, $m_3 = 25$; $\rho_{1,2} = 0.09$, $\rho_{1,3} = -0.42$, $\rho_{2,3} = 0.20$.

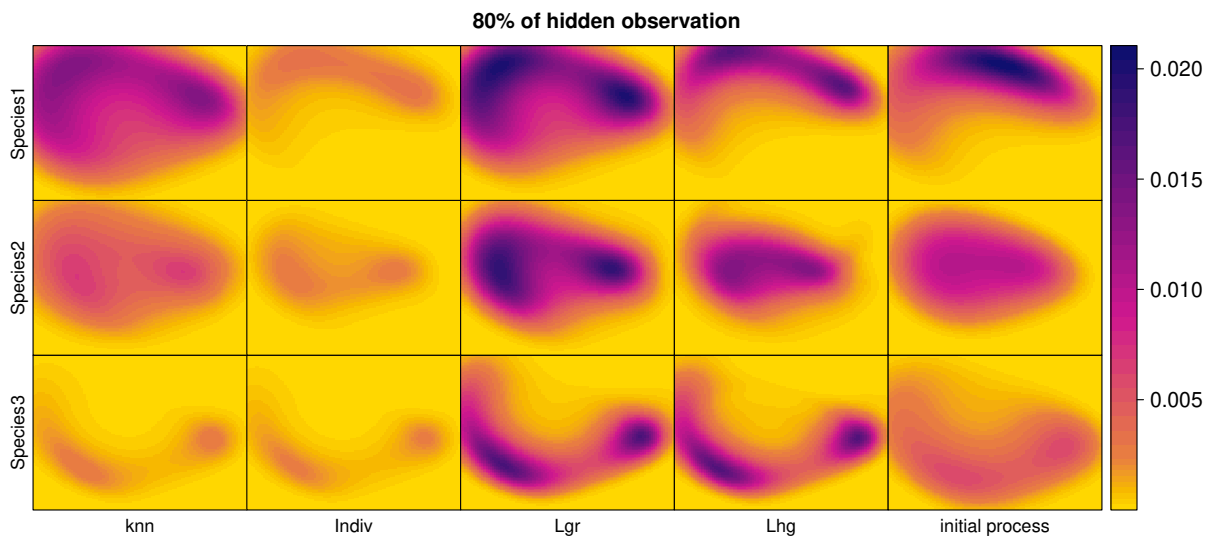


Figure 8: Predicted intensities obtained for the knn, individual, Loop grW and Loop hgW methods and the initial intensities from the process with 80% of hidden observations. The parameters of abundances and correlation are: $m_1 = 42$, $m_2 = 31$, $m_3 = 25$; $\rho_{1,2} = 0.09$, $\rho_{1,3} = -0.42$, $\rho_{2,3} = 0.20$.

5.1.4 Similar abundances and non-correlated distribution

275 For similar abundances ($m_1 = 39$, $m_2 = 37$, $m_3 = 38$) and non correlated distributions, we again observe
 276 the same trends, as shown in Figure 9: the knn method is the worst method for relabeling performances
 277 and the only one not doing as well as the individual method for 50% and 80% of hidden observations.
 278 As in previous contexts, the Loop grW method shows the best predictive performance, with the Loop
 279 hgW method being competitive with the individual PPM method, and the knn method having higher
 280 IMSE than the other methods when 80% of the observations are hidden. Tables 7 and 8 in the Appendix
 281 contain the mean and median value for all performance measures.
 282 The predicted intensities show the methods LgrW and knn being the closest to the initial process, as
 283 shown in Figure 10.

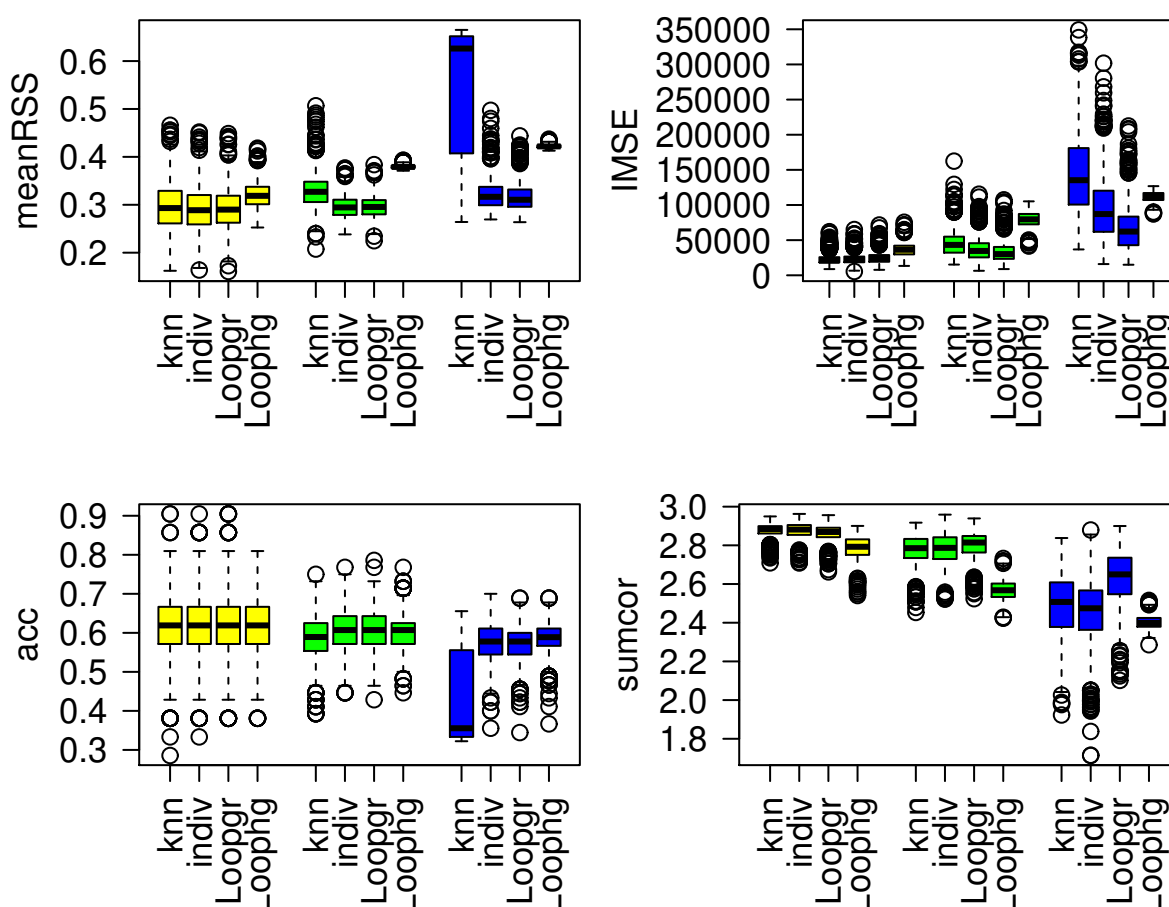


Figure 9: Measures of performance for the knn, individual, Loop grW and Loop grW methods. Each color represents a different proportion of hidden observations: in yellow are the performances with 20% of hidden observations, in green with 50% and in blue with 80%. The parameters of abundances and correlation are: $m_1 = 39$, $m_2 = 37$, $m_3 = 38$; $\rho_{1,2} = 0.09$, $\rho_{1,3} = -0.42$, $\rho_{2,3} = 0.20$.

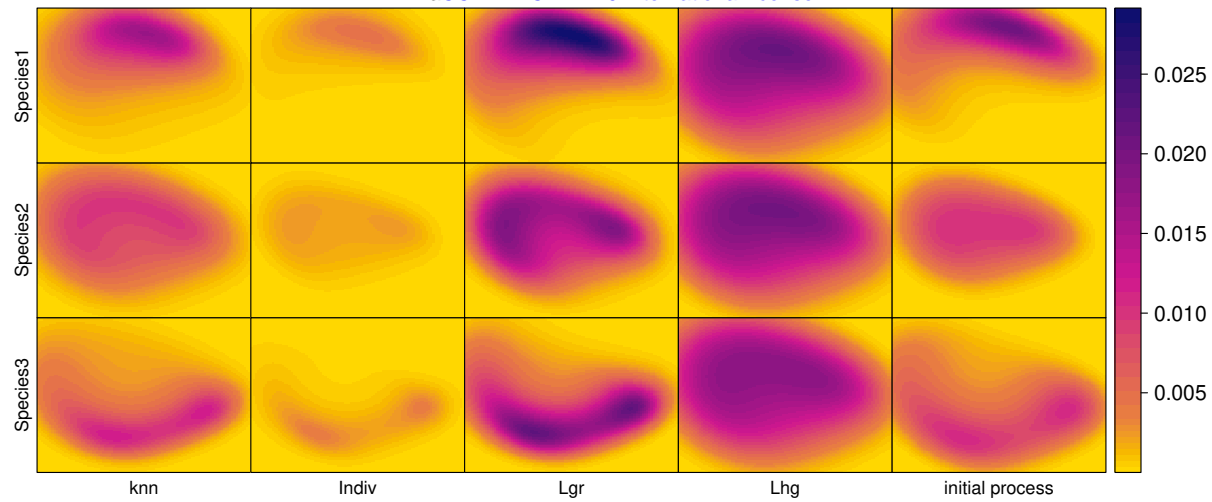


Figure 10: Predicted intensities obtained for the knn, individual, Loopg rW and Loop grW initialization methods and the initial intensities from the process at 80% of hidden observations. The parameters of abundances and correlation are: $m_1=39$, $m_2=37$, $m_3=38$; $\rho_{1-2}=0.09$, $\rho_{1-3}=-0.42$, $\rho_{2-3}=0.20$

284 5.2 Testing algorithm parameters

285 5.2.1 knn method

286 We note that when the k nearest neighbor value increases (from 1 up to 20), the model performances
287 decrease; Figure 11. It is particularly notable for the performances in prediction where sumcor performances
288 decrease and IMSE performances increase. Also, there is an expected drop in performances as we increase
289 the proportion of observations with unknown species labels.

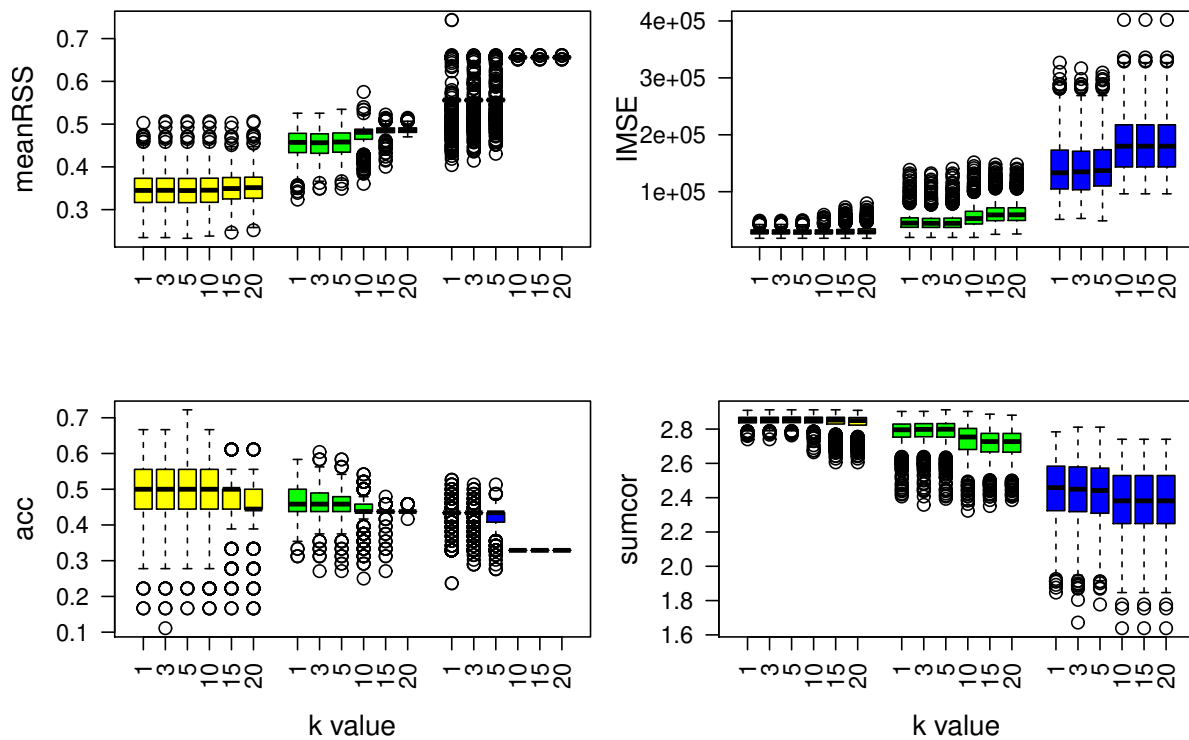


Figure 11: Model performances for the knn method. Each color represents a different percentage of hidden observations: in yellow are the performances with 20% of hidden observations, in green with 50% and in blue with 80%. The parameters of abundances and correlation are: $m_1 = 32$, $m_2 = 42$, $m_3 = 23$; $\rho_{1,2} = 0.85$, $\rho_{1,3} = -0.09$, $\rho_{2,3} = 0.20$

290 5.2.2 Loop grW method

291 For the Loop grW method we tested different parameters:

- 292 1. The initial membership probability threshold δ_{\max} : while this parameter varies from 0.8 to 0.5 in
293 increments of 0.1, the other Loop grW parameters are as follows: $\delta_{\min} = 0.1$ and $\delta_{\text{step}} = 0.1$.
- 294 2. The final membership probability threshold δ_{\min} : while this parameter varies from 0.1 to 0.7 in
295 increments of 0.2, the other Loop grW parameters are as follows: $\delta_{\max} = 0.8$ and $\delta_{\text{step}} = 0.1$.
- 296 3. The step size δ_{step} : while this parameter varies from a minimum of 0.01 to a maximum of 0.2, the
297 other Loop grW parameters are as follows: $\delta_{\max} = 0.8$ and $\delta_{\min} = 0.1$.

298 When we change the value of δ_{\max} , there is very little difference in performance within each proportion of
299 observations with hidden labels, although $\delta_{\max} = 0.5$ appears to be slightly superior to the other choices
300 for high percentage of hidden observation (Figure 12).

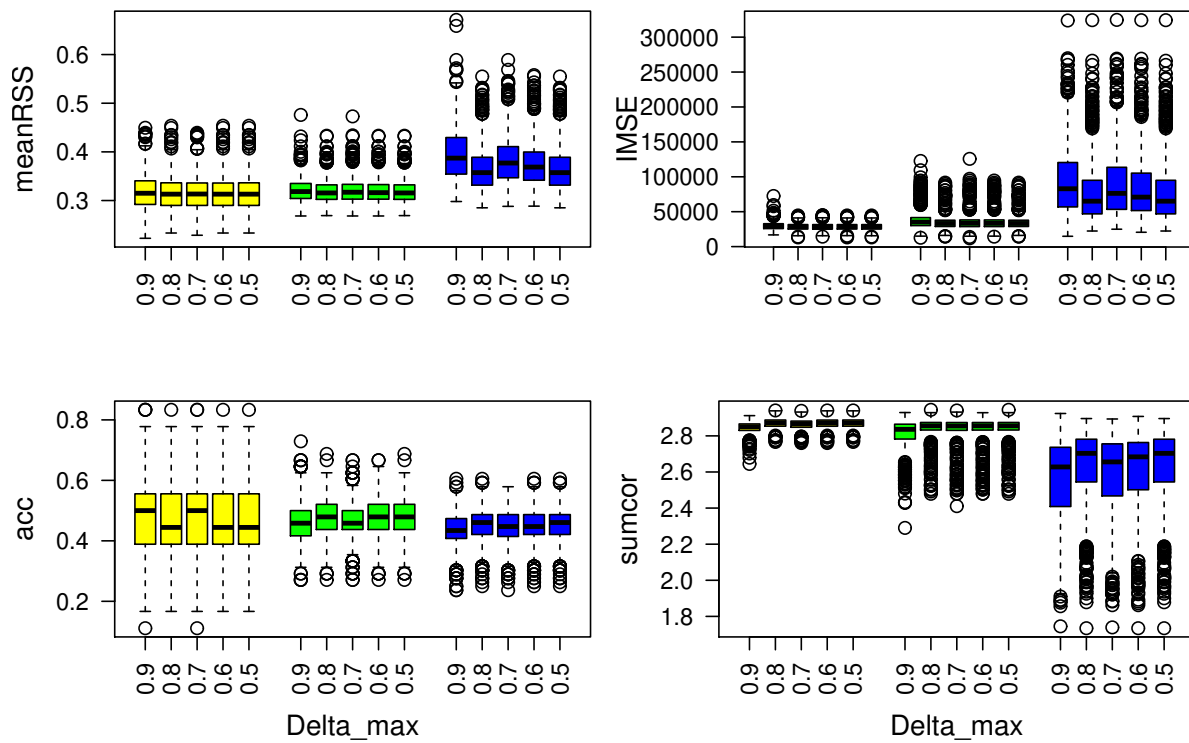


Figure 12: Model performances for the Loop grW method and for different values of δ_{\max} . Each color represents a different proportion of hidden observations: in yellow are the performances with 20% of hidden observations, in green with 50% and in blue with 80%. The parameters of abundances and correlation are: $m_1 = 32$, $m_2 = 42$, $m_3 = 23$; $\rho_{1,2} = 0.85$, $\rho_{1,3} = -0.09$, $\rho_{2,3} = 0.20$

301 When changing δ_{\min} , the classification accuracy is relatively the same (Figure 13). For MeanRSS, IMSE
 302 and sumcor, we can observe a curved pattern of performances, where the performances decrease (MeanRSS
 303 increases, IMSE increases and sumcor decreases) from δ_{\min} from 0.1 to 0.5 and then the performances get
 304 slightly better (MeanRSS decreases, IMSE decreases and sumcor increases) for $\delta_{\min} = 0.7$ (Figure 13).
 305 $\delta_{\min}=0.1$ displays the better performances.

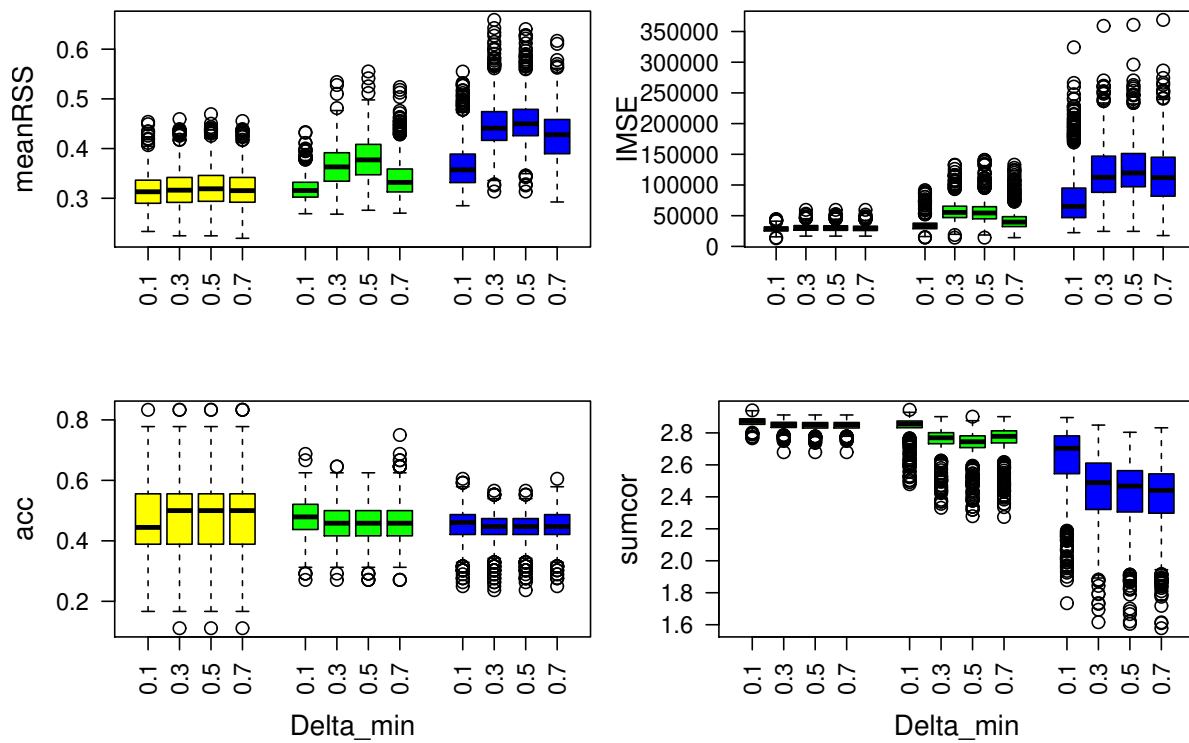


Figure 13: Model performances for the Loop grW method and for different values of δ_{\min} . Each color represents a different proportion of hidden observations: in yellow are the performances with 20% of hidden observations, in green with 50% and in blue with 80%. The parameters of abundances and correlation are: $m_1 = 32$, $m_2 = 42$, $m_3 = 23$; $\rho_{1,2} = 0.85$, $\rho_{1,3} = -0.09$, $\rho_{2,3} = 0.20$

306 Figure 14 shows different performance measures as we vary δ_{step} . There do not appear to be major
 307 differences in classification performance, although 0.1 appear slightly better for meanRSS. With 50% and
 308 80% of hidden observations, predictive performance display a curve performances where performances get
 309 better (IMSE decreases and sumcor increase) from 0.01 till 0.1 and then get worse (IMSE increases and
 310 sumcor decreases) from 0.1 to 0.2. $\delta_{\text{step}}=0.1$ displays the best performances across all measures.

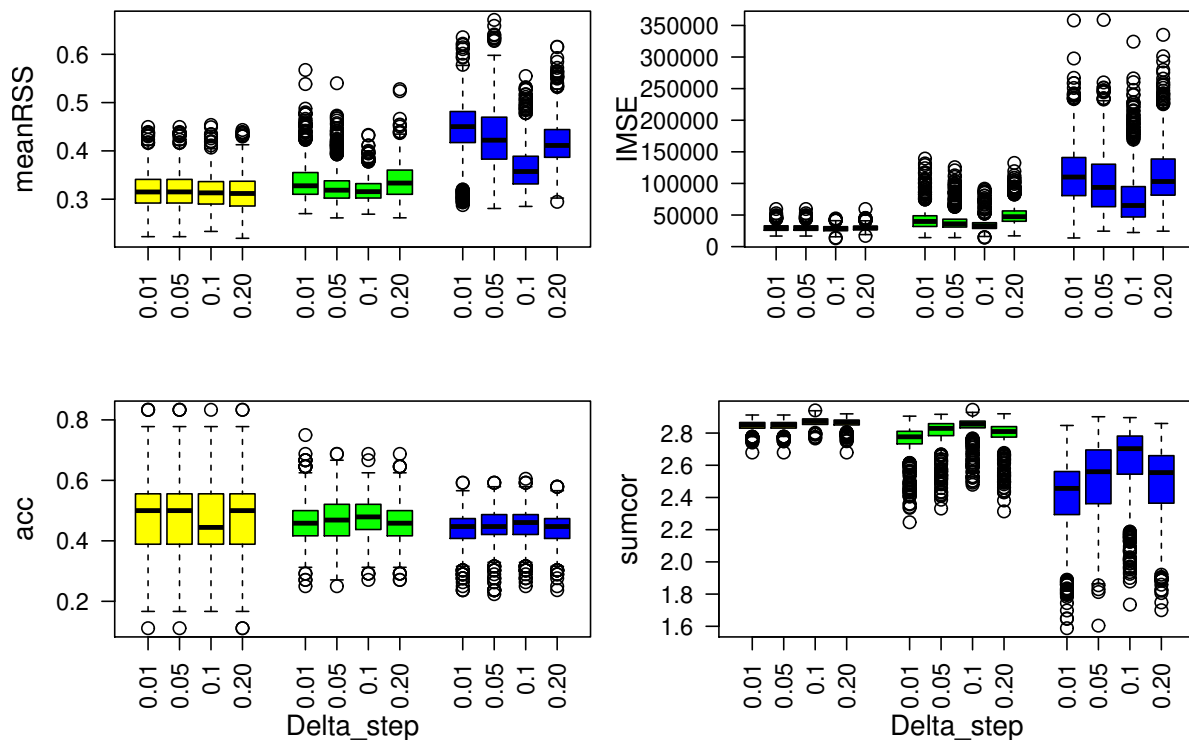


Figure 14: Model performances for the Loop grW method and for different values of weight step. Each color represents a different proportion of hidden observations: in yellow are the performances with 20% of hidden observations, in green with 50% and in blue with 80%. The parameters of abundances and correlation are: $m_1 = 32$, $m_2 = 42$, $m_3 = 23$; $\rho_{1,2} = 0.85$, $\rho_{1,3} = -0.09$, $\rho_{2,3} = 0.20$

311 5.2.3 Loop hgW method

312 In the Loop hgW method, we vary the number of points a added at each iteration. In Figure 15, we can
 313 see that there is no variation in performances when the number of added points a increases.

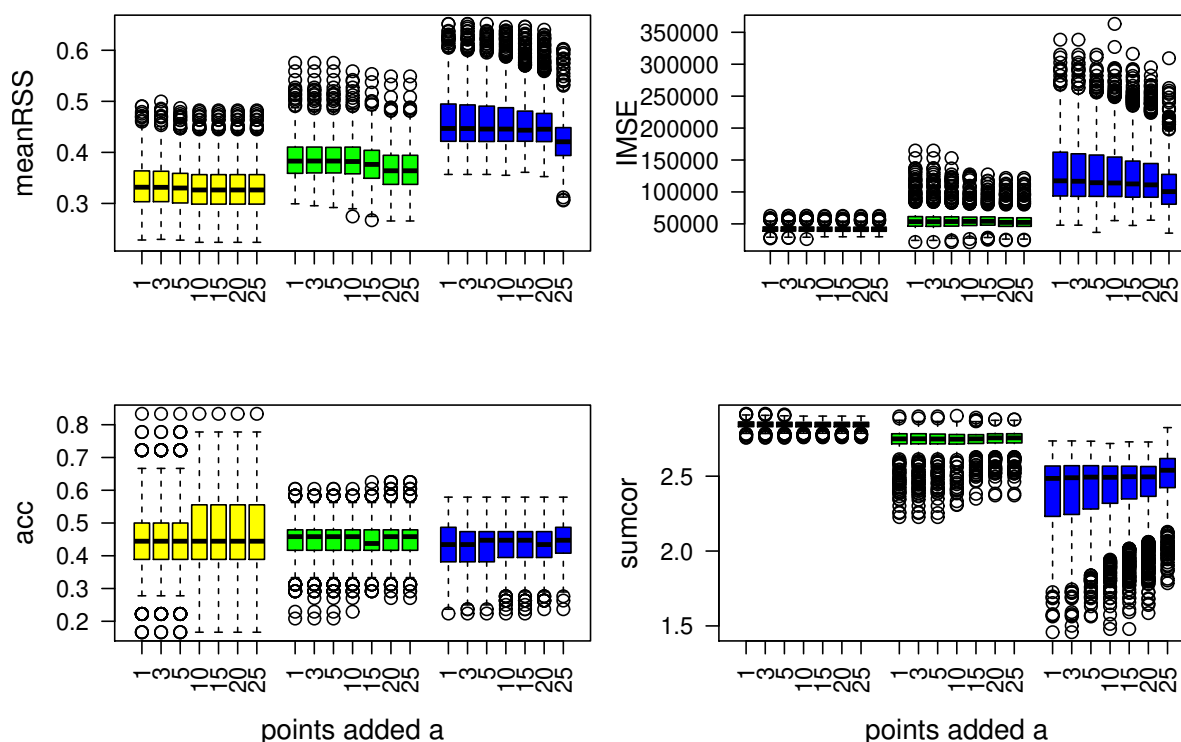


Figure 15: Model performances for the Loop grW method. Each color boxplot represents a different percentage of hidden observations: in yellow are the performances for 20% of hidden observations, in green for 50% and in blue for 80%. The parameters of abundances and correlation are: $m_1 = 32$, $m_2 = 42$, $m_3 = 23$; $\rho_{1,2} = 0.85$, $\rho_{1,3} = -0.09$, $\rho_{2,3} = 0.20$

314 The results for the other combination of abundances and correlation are showed in the Appendix.

315 6 Discussion

316 In this article, we present a new modelling tool in R that aims to incorporate the observed locations
 317 with unknown species identities to improve species distributions. These tools accommodate two ways of
 318 reclassifying information using mixture modelling and the machine learning framework with 7 different
 319 initialization methods. We tested our algorithms in different contexts where we vary the abundances of
 320 our species (similar or different), the correlation between them (two distribution are correlated or none are
 321 correlated) and the proportion of unknown species identities (20%, 50% and 80%). The different methods
 322 were compared to the individual method which ignores locations with unknown species identities to see
 323 whether the proposed algorithms allow us to fit distributions that are closer to the initial processes.

324 In the results we presented the three best methods. They showed varying performance depending on
 325 the aspects of the model and the performance measure considered. The novelty of these tools, makes it
 326 difficult to compare to other existing tools that either do not consider point pattern process (Frame &
 327 Jammalamadaka, 2007; Frühwirth-Schnatter, 2006; Hui, 2016; Martinez, 2015; Melnykov & Maitra, 2010;
 328 Quost & Dencœur, 2016), Poisson distributions (Figueirido & Jain, 2002; Hui *et al.*, 2015; Scrucca *et al.*,

329 of mixture (Witten, 2011; Wendel *et al.*, 2015) or semi-supervised learning frameworks (Di Zio *et al.*, 2007;
330 Fraley & Raftery, 1998; Jeffries & Pfeiffer, 2001; Taddy & Kottas, 2012).

331 The other methods (kmeans, random, equal and normal) not presented previously in the results are
332 presented in the Appendix. They show relatively worse performance across all measures, although at
333 times, the normal loop method is competitive with the individual PPM and the Loop hgW methods. We
334 note that this method performs slightly better when the distributions are correlated.
335

336 We have noticed differences in performance, that are more significant when we increase the proportion
337 of observations with hidden labels. While at 20% of hidden observations, all methods performed fairly
338 similarly, at 50% and 80% of hidden observations, the loop grW method in particular showed the best
339 predictive performances regardless of differences in abundance and correlation among species distributions.
340 For this method, only the points with the highest membership probabilities are added. We set the
341 maximum and minimum thresholds at $\delta_{\max} = 0.5$ and $\delta_{\min} = 0.1$ and a step size of $\delta_{\text{step}} = 0.1$, but we
342 could expect that performances may be better or worse with different choices of these parameters as
343 shown in the results. These choices appeared to produce superior performances for most measures than
344 other values of these parameters considered. Higher values of δ_{\min} led to worse performances. This result
345 can be seen as counterintuitive as we can expect that having a smaller interval of weight for example could
346 improve this particular performances. It will in other words reduce the interval of weights and better
347 discriminate the points of uncertain identity. As for δ_{step} , choosing a value that is too small may lead to
348 iterations where no points are added, while choosing a value that is too large may be too discriminating
349 and does not allow to reclassify the points.

350 The Loop hgW method did not perform as good as the Loop grW method even if it has been shown to be
351 as good as the individual method in some contexts. For this method, we add initially a certain number of
352 points a that is increased at each iteration. While the a points with highest membership probabilities are
353 added, these membership probabilities may be small for large values of a , and this could explain that this
354 method is not always doing as good as the best method.

355 Interestingly, the knn method was the best of the four mixture methods tested, outperforming the kmeans,
356 random and equal initialization options. Previous studies using the EM algorithm for classification and
357 clustering data show that such algorithms are highly dependent on the initialization method (Figueirido
358 & Jain, 2002; Melnykov & Maitra, 2010; O'Hagan *et al.*, 2012). Additionally, even very popular methods
359 like kmeans have some drawbacks. Its performance is dependent on overlapping densities and whether the
360 distributions are roughly circular or not. The choice of the centroid is also not consistent and chosen at
361 random for the first calculation (Yoo *et al.*, 2012, 2007; Wu *et al.*, 2008). In our simulations, kmeans,
362 random and equal methods showed very different results and always performed worse than the other

364 intensities compared to the true process.

365 Despite outperforming the other mixture modelling methods, the knn method was still not competitive
366 with the machine learning methods or the individual PPM method when the proportion of hidden
367 observations are 50% or 80%. However, the knn method was quite consistent in the predicted intensities
368 and showed similar results to the individual method for the sumcor measure at 50% or 80% of hidden
369 observations. Other studies have found that the performance of the knn method is linked to the metric
370 chosen to calculate the nearest neighbor distances and the value of the number k of nearest neighbors
371 (Weinberger & Saul, 2009; Guo *et al.*, 2003; Wu *et al.*, 2008).

372 We tested how the number of neighbors k can influence the model and found that for any combination of
373 abundance and correlation, all the measures of performances decrease when the values of k increase. It is
374 expected as the neighboring points are further away from one another and could conflate species habitat
375 preferences with differing species abundances, but requiring more neighbor points can also stabilize the
376 distances. The way of choosing the value of k by utilizing different distance metrics could also impact the
377 performances as previously noted, but we shall leave this aspect of the analysis for future consideration.

378 In our simulations, we have considered a relatively general case of point patterns and we only varied
379 species abundance and correlation among distributions in addition to the proportion of observations with
380 hidden information. For real ecological data sets, there are more factors to consider that can influence
381 how a model will perform. First, the abundances tested in the simulation are quite low (20-40 points) and
382 some methods can show convergence issues in this context. While we use the spatstat package (Baddeley
383 *et al.*, 2015) to fit PPMs, we could make use of similar functions in the ppmlasso package (Renner &
384 Warton, 2013) which integrate regularization methods like the lasso penalty that can boost performances
385 with low sample sizes. A related point is that we included all covariates that were used to generate
386 the true point patterns in our models. In real situations, however, we may not have access to the best
387 covariates or know which ones truly determine the species distributions. Applying a lasso penalty to help
388 in variable selection may therefore be provide a natural way forward in this context. Finally, a key reality
389 when dealing with presence-only data is the presence of observer bias, in which sampling effort varies
390 throughout the study region. Some models apply a correction for observer bias in the prediction (Hefley
391 *et al.*, 2013; Lahoz-Monfort *et al.*, 2014; Warton *et al.*, 2013) and our tools would be able to accommodate
392 such improvements.

393 7 Conclusion

394 The new algorithms presented in this article aim to reclassify observations that have uncertain or unknown
395 labels in order to better predict point pattern distributions. We showed that machine learning based

397 method and also better than the individual PPM method that does not include the points with unknown
398 labels. Our simulations showed encouraging results in this context with good performances in some cases,
399 although there are some improvements to implement in order to make the tools more appropriate for real
400 life data.



401 Acknowledgments

402 Computational resources used in this work were provided by Intersect Australia Ltd.

403 Authors' contributions

404 EG and IR conceived the ideas and designed methodology; EG and IR built the algorithms; EG analyzed
405 the data; EG and IR led the writing of the manuscript. MM had an overview on the project. MM and EB
406 reviewed the paper. All authors contributed critically to the drafts and gave final approval for publication.

407 Data accessibility

408 Rscript: An example of the scripts used for this paper is available here: functions to use for the test
409 simulation  and the script example .

410 References

- 411 Aarts, G., Fieberg, J. & Matthiopoulos, J. (2012) Comparative interpretation of count, presence-absence
412 and point methods for species distribution models. *Methods in Ecology and Evolution*, **3**, 177–187.
413 <https://doi.org/10.1111/j.2041-210X.2011.00141.x>.
- 414 Baddeley, A., Gregori, P., Mateu, J., Stoica, R. & Stoyan, D. (2006) *Modelling Spatial Point Patterns*
415 *in R*. In: *Baddeley A., Gregori P., Mateu J., Stoica R., Stoyan D. (eds) Case Studies in Spatial*
416 *Point Process Modeling.*, volume 185 of *Lecture Notes in Statistics*. Springer, New York, NY. https://doi.org/10.1007/0-387-31144-0_2.
- 418 Baddeley, A., Rubak, E. & Turner, R. (2015) *Spatial Point Patterns: Methodology and Applications with*
419 *R*. Chapman and Hall/CRC Press, London. <https://doi.org/10.1201/b19708>.
- 420 Benaglia, T., Chauveau, D., Hunter, D.R. & Young, D. (2009) mixtools: An R package for analyzing
421 finite mixture models. *Journal of Statistical Software*, **32**, 1–29. <https://doi.org/10.18637/jss.v032.i06>.
- 422 Berman, M. & Turner, T.R. (1992) Approximating point process likelihoods with glim. *Journal of the*
423 *Royal Statistical Society: Series C (Applied Statistics)*, **41**, 31–38. <https://doi.org/10.2307/2347614>.

- 424 Browning, E., Bolton, M., Owen, E., Shou, A., Gaultford, L., Freeman, R. & McPherson, J. (2018)
425 Predicting animal behaviour using deep learning: Gps data alone accurately predict diving in seabirds.
426 *Methods in Ecology and Evolution*, **9**, 681–692. <https://doi.org/10.1111/2041-210x.12926>.
- 427 Burnham, K.P. & Anderson, D.R. (2002) *Model Selection and Multimodel Inference: A Practical*
428 *Information-Theoretic Approach*. Springer, New York, NY, 2 edition. <https://doi.org/10.1007/b97636>.
- 429 Di Zio, M., Guarnera, U. & Rocci, R. (2007) A mixture of mixture models for a classification problem:
430 The unity measure error. *Computational Statistics and Data Analysis*, **51**, 2573–2585. <https://doi.org/10.1016/j.csda.2006.01.001>.
- 432 Dunstan, P.K., Foster, S.D., Hui, F.K.C. & Warton, D.I. (2013) Finite mixture of regression modeling
433 for high-dimensional count and biomass data in ecology. *Journal of Agricultural, Biological, and*
434 *Environmental Statistics*, **18**, 357–375. <https://doi.org/10.1007/s13253-013-0146-x>.
- 435 Es, B. (1997) A note on the integrated squared error of a kernel density estimator in non-smooth cases.
436 *Statistics and Probability Letters*, **35**, 241–250. [https://doi.org/10.1016/S0167-7152\(97\)00019-9](https://doi.org/10.1016/S0167-7152(97)00019-9).
- 437 Fernández-Michelli, J.I., Hurtado, M., Areta, J.A. & Muravchik, C.H. (2016) Unsupervised classification
438 algorithm based on em method for polarimetric sar images. *ISPRS Journal of Photogrammetry and*
439 *Remote Sensing*, **117**, 56–65. <https://doi.org/10.1016/j.isprsjprs.2016.03.001>.
- 440 Figueirido, M.A. & Jain, A.K. (2002) Unsupervised learning of finite mixture models. *IEEE Transactions*
441 *on pattern analysis and machine intelligence*, **24**, 381–396. <https://doi.org/10.1109/34.990138>.
- 442 Fraley, C. & Raftery, A.E. (1998) How many clusters? which clustering method? answers via model-based
443 cluster analysis. *The computer journal*, **41**, 578–588. <https://doi.org/10.1093/comjnl/41.8.578>.
- 444 Frame, S.J. & Jammalamadaka, S.R. (2007) Generalized mixture models, semi-supervised learning, and
445 unknown class inference. *Advances in Data Analysis and Classification*, **1**, 23–38. <https://doi.org/10.1007/s11634-006-0001-9>.
- 447 Franklin, J. (2013) Species distribution models in conservation biogeography: developments and challenges.
448 *Diversity and Distributions*, **19**, 1217–1223. <https://doi.org/10.1111/ddi.12125>.
- 449 Frühwirth-Schnatter, S. (2006) *Finite mixture and Markov switching models*. Springer series in statistics.
450 Springer. <https://doi.org/10.1007/978-0-387-35768-3>.
- 451 Guillera-Arroita, G., Lahoz-Monfort, J.J., Elith, J., Gordon, A., Kujala, H., Lentini, P.E., McCarthy,
452 M.A., Tingley, R. & Wintle, B.A. (2015) Is my species distribution model fit for purpose? matching
453 data and models to applications. *Global Ecology and Biogeography*, **24**, 276–292. <https://doi.org/10.1111/geb.12268>.
- 455 Guisan, A., Tingley, R., Baumgartner, J.B., Naujokaitis-Lewis, I., Sutcliffe, P.R., Tulloch, A.I., Regan,

- 456 I.J., Brotons, L., McDonald-Madden, K., Manlyka, Pringle, C., Martin, T.G., Rhodes, J.R., Maggini,
457 R., Setterfield, S.A., Elith, J., Schwartz, M.W., Wintle, B.A., Broennimann, O., Austin, M., Ferrier,
458 S., Kearney, M.R., Possingham, H.P. & Buckley, Y.M. (2013) Predicting species distributions for
459 conservation decisions. *Ecol Lett*, **16**, 1424–35. <https://doi.org/10.1111/ele.12189>.
- 460 Guo, G., Wang, H., Bell, D., Bi, Y. & Greer, K. (2003) Knn model-based approach in classification.
461 R. Meersman, Z. Tari & D.C. Schmidt, eds., *On The Move to Meaningful Internet Systems 2003:
462 CoopIS, DOA, and ODBASE*, pp. 986–996. Springer Berlin Heidelberg, Berlin, Heidelberg. https://doi.org/10.1007/978-3-540-39964-3_62.
- 464 Hastie, T., Tibshirani, R. & Friedman, J. (2001) *The Elements of Statistical Learning Data Mining, In-
465 ference, and Prediction*, volume 1. Springer, New York, NY. <https://doi.org/10.1007/978-0-387-21606-5>.
- 466 Hefley, T.J., Tyre, A.J., Baasch, D.M. & Blankenship, E.E. (2013) Nondetection sampling bias in marked
467 presence-only data. *Ecol Evol*, **3**, 5225–36. <https://doi.org/10.1002/ece3.887>.
- 468 Hui, F.K.C. (2016) *Mixing it Up: New Methods for Finite Mixture Modelling of Multi-Species Data in
469 Ecology*. Ph.D. thesis. <https://doi.org/10.1017/S0004972715000945>.
- 470 Hui, F.K.C., Warton, D.I. & Foster, S.D. (2015) Multi-species distribution modeling using penalized
471 mixture of regressions. *The Annals of Applied Statistics*, **9**, 866–882. <https://doi.org/10.1214/15-aos813>.
- 472 Illian, J.B., Sørbye, S.H. & Rue, H. (2012) A toolbox for fitting complex spatial point process models
473 using integrated nested laplace approximation (inla). *The Annals of Applied Statistics*, **6**, 1499–1530.
474 <https://doi.org/10.1214/11-aos530>.
- 475 Inoue, K., Stoeckl, K., Geist, J. & Ricciardi, A. (2017) Joint species models reveal the effects of environment
476 on community assemblage of freshwater mussels and fishes in european rivers. *Diversity and Distributions*,
477 **23**, 284–296. <https://doi.org/10.1111/ddi.12520>.
- 478 Iovleff, S. (2018) *MixAll: Clustering and Classification using Model-Based Mixture Models*. R package
479 version 1.4.2.
- 480 Jeffries, N. & Pfeiffer, R. (2001) A mixture model for the probability distribution of rain rate. *Environ-
481 metrics*, **12**, 1–10. [https://doi.org/10.1002/1099-095X\(200102\)12:1<1::AID-ENV425>3.0.CO;2-N](https://doi.org/10.1002/1099-095X(200102)12:1<1::AID-ENV425>3.0.CO;2-N).
- 482 Jewell, K.J., Arcese, P. & Gergel, S.E. (2007) Robust predictions of species distribution: Spatial habitat
483 models for a brood parasite. *Biological Conservation*, **140**, 259–272. <https://doi.org/10.1016/j.biocon.2007.08.017>.
- 484
485 Lahoz-Monfort, J.J., Guillera-Arroita, G. & Wintle, B.A. (2014) Imperfect detection impacts the per-
486 formance of species distribution models. *Global Ecology and Biogeography*, **23**, 504–515. <https://doi.org/10.1111/geb.12138>.
- 487

- 488 Lersch, P. (2004) FlexMix: A general framework for finite mixture models and latent class regression in R.
489 *Journal of Statistical Software*, **11**, 1–18. <https://doi.org/10.18637/jss.v011.i08>.
- 490 Mahony, M., Donnellan, S.C., Richards, S.J. & Donald, K. (2006) Species boundaries among barred river
491 frogs, mixophyes (anura: Myobatrachidae) in north-eastern australia, with descriptions of two new
492 species. *Zootaxa*, **1228**, 35–60. <https://doi.org/10.5281/zenodo.172713>.
- 493 Martinez, D.F. (2015) *Mixture-based Clustering for the Ordered Stereotype Model*. Thesis, School of
494 Mathematics Statistics and Operations Research. <https://doi.org/10.13140/RG.2.1.1945.4806>.
- 495 Matthews, J., Steiner, L. & Gordon, J. (2001) Mark-recapture analysis of sperm whale (physeter macro-
496 cephalus) photo-id data from the azores (1987-1995). *Journal of cetacean research and management*, **3**,
497 219–226.
- 498 McLachlan, G.J. & Peel, D. (2000) *Finite Mixture Models*. Wiley, New York. [https://doi.org/10.1002/](https://doi.org/10.1002/0471721182)
499 [0471721182](https://doi.org/10.1002/0471721182).
- 500 Melnykov, V. & Maitra, R. (2010) Finite mixture models and model-based clustering. *Statistics Surveys*,
501 **4**, 80–116. <https://doi.org/10.1214/09-ss053>.
- 502 Mi, X., Bao, L., Jianhua, C. & Ma, K. (2014) Point process models, the dimensions of biodiversity
503 and the importance of small-scale biotic interactions. *Journal of Plant Ecology*, **7**, 126–133. <https://doi.org/10.1093/jpe/rtt075>.
- 504
- 505 Nezer, O., Bar-David, S., Gueta, T. & Carmel, Y. (2016) High-resolution species-distribution model
506 based on systematic sampling and indirect observations. *Biodiversity and Conservation*, **26**, 421–437.
507 <https://doi.org/10.1007/s10531-016-1251-2>.
- 508 O’Hagan, A., Murphy, T.B. & Gormley, I.C. (2012) Computational aspects of fitting mixture models via
509 the expectation–maximization algorithm. *Computational Statistics and Data Analysis*, **56**, 3843–3864.
510 <https://doi.org/10.1016/j.csda.2012.05.011>.
- 511 Peterman, W.E., Crawford, J.A. & Kuhns, A.R. (2013) Using species distribution and occupancy modeling
512 to guide survey efforts and assess species status. *Journal for Nature Conservation*, **21**, 114–121.
513 <https://doi.org/10.1016/j.jnc.2012.11.005>.
- 514 Quost, B. & Dencœur, T. (2016) Clustering and classification of fuzzy data using the fuzzy em algorithm.
515 *Fuzzy Sets and Systems*, **286**, 134–156. <https://doi.org/10.1016/j.fss.2015.04.012>.
- 516 R Core Team (2017) *R: A Language and Environment for Statistical Computing*. R Foundation for
517 Statistical Computing, Vienna, Austria. <https://www.R-project.org/>.
- 518 Renner, I.W., Elith, J., Baddeley, A., Fithian, W., Hastie, T., Phillips, S.J., Popovic, G., Warton, D.I. &
519 O’Hara, R.B. (2015) Point process models for presence-only analysis. *Methods in Ecology and Evolution*,

- 521 Renner, I.W. & Warton, D.I. (2013) Equivalence of maxent and poisson point process models for species
522 distribution modeling in ecology. *Biometrics*, **69**, 274–281. [https://doi.org/10.1111/j.1541-0420.2012.](https://doi.org/10.1111/j.1541-0420.2012.01824.x)
523 01824.x.
- 524 Ruete, A. & Leynaud, G.C. (2015) Goal-oriented evaluation of species distribution models' accuracy
525 and precision: True skill statistic profile and uncertainty maps. Technical report, PeerJ PrePrints.
526 <https://dx.doi.org/10.7287/peerj.preprints.1208v1>.
- 527 Schank, C.J., Cove, M.V., Kelly, M.J., Mendoza, E., O'Farrill, G., Reyna-Hurtado, R., Meyer, N., Jordan,
528 C.A., González-Maya, J.F., Lizcano, D.J., Moreno, R., Dobbins, M.T., Montalvo, V., Sáenz-Bolaños,
529 C., Jimenez, E.C., Estrada, N., Cruz Díaz, J.C., Saenz, J., Spínola, M., Carver, A., Fort, J., Nielsen,
530 C.K., Botello, F., Pozo Montuy, G., Rivero, M., de la Torre, J.A., Brenes-Mora, E., Godínez-Gómez,
531 O., Wood, M.A., Gilbert, J., Miller, J.A. & Thuille, W. (2017) Using a novel model approach to assess
532 the distribution and conservation status of the endangered baird's tapir. *Diversity and Distributions*,
533 **23**, 1459–1471. <https://doi.org/10.1111/ddi.12631>.
- 534 Scrucca, L., Fop, M., Murphy, T.B. & Raftery, A.E. (2016) mclust 5: Clustering, classification and density
535 estimation using gaussian finite mixture models. *the R journal*, **8**, 289–317. [https://doi.org/10.21236/](https://doi.org/10.21236/ada459792)
536 ada459792.
- 537 Swanepoel, J.W.H. (1988) Mean intergrated squared error properties and optimal kernels when estimating
538 a distribution function. *Communications in Statistics - Theory and Methods*, **17**, 3785–3799. <https://doi.org/10.1080/03610928808829835>.
- 540 Taddy, M.A. & Kottas, A. (2012) Mixture modeling for marked poisson processes. *Bayesian Analysis*, **7**,
541 335–362. <https://doi.org/10.1214/12-ba711>.
- 542 Thessen, A. (2016) Adoption of machine learning techniques in ecology and earth science. *One Ecosystem*,
543 **1**. <https://doi.org/10.3897/oneeco.1.e8621>.
- 544 Tracey, J.A., Zhu, J., Boydston, E., Lyren, L., Fisher, R.N. & Crooks, K.R. (2013) Mapping behavioral
545 landscapes for animal movement: a finite mixture modeling approach. *Ecological Applications*, **23**,
546 654–669. <https://doi.org/10.1890/12-0687.1>.
- 547 Tran, N.Q. (2017) *Classification, Novelty Detection and Clustering for Point Pattern Data*. Thesis,
548 Faculty of Science and Engineering, Department of Electrical and Computer Engineering. <http://hdl.handle.net/20.500.11937/59025>.
- 550 van Strien, A.J., van Swaay, C.A. & Termaat, T. (2013) Opportunistic citizen science data of animal
551 species produce reliable estimates of distribution trends if analysed with occupancy models. *Journal of*
552 *Applied Ecology*, **50**, 1450–1458. <https://doi.org/10.1111/1365-2664.12158>.

- 553 Vo, B.N., Dam, N., Phung, D., N. Lee, Q., & Vo, B.T. (2018) Model-based learning for point pattern
554 data. *Pattern Recognition*, **84**. <https://doi.org/10.1016/j.patcog.2018.07.008>.
- 555 Warton, D.I., Renner, I.W. & Ramp, D. (2013) Model-based control of observer bias for the analysis of
556 presence-only data in ecology. *PLoS One*, **8**, e79168. <https://doi.org/10.1371/journal.pone.0079168>.
- 557 Warton, D.I. & Shepherd, L.C. (2010) Poisson point process models solve the “pseudo-absence problem”
558 for presence-only data in ecology. *The Annals of Applied Statistics*, **4**, 1383–1402. <https://doi.org/10.1214/10-aos331>.
- 559
- 560 Weinberger, K.Q. & Saul, L.K. (2009) Distance metric learning for large margin nearest neighbor
561 classification. *Journal of Machine Learning Research*, **10**, 207–244. <https://doi.org/10.1145/1577069.1577078.21,38>.
- 562
- 563 Wendel, J., Buttenfield, B.P. & Stanislawski, L.V. (2015) An evaluation of unsupervised and supervised
564 learning algorithms for clustering landscape types in the united states. *Cartography and Geographic
565 Information Science*, **43**, 233–249. <https://doi.org/10.1080/15230406.2015.1067829>.
- 566 Witten, D.M. (2011) Classification and clustering of sequencing data using a poisson model. *The Annals
567 of Applied Statistics*, **5**, 2493–2518. <https://doi.org/10.1214/11-aos493>.
- 568 Woillez, M., Ressler, P.H., Wilson, C.D. & Horne, J.K. (2012) Multifrequency species classification of
569 acoustic-trawl survey data using semi-supervised learning with class discovery. *J Acoust Soc Am*, **131**,
570 EL184–90. <https://doi.org/10.1121/1.3678685>.
- 571 Wu, X., Kumar, V., Quinlan, J.R., Ghosh, J., Yang, Q., Motoda, H., McLachlan, G.J., Ng, A., Liu, B.,
572 Philip, S.Y. *et al.* (2008) Top 10 algorithms in data mining. *Knowledge and information systems*, **14**,
573 1–37. <https://doi.org/10.1007/s10115-007-0114-2>.
- 574 Yoo, I., Alafaireet, P., Marinov, M., Pena-Hernandez, K., Gopidi, R., Chang, J.F. & Hua, L. (2012) Data
575 mining in healthcare and biomedicine: A survey of the literature. *Journal of Medical Systems*, **36**,
576 2431–2448. [10.1007/s10916-011-9710-5](https://doi.org/10.1007/s10916-011-9710-5).
- 577 Yoo, I., Hu, X. & Song, I.Y. (2007) Biomedical ontology improves biomedical literature clustering
578 performance: a comparison study. *International Journal of Bioinformatics Research and Applications*,
579 **3**, 414–428. <https://doi.org/10.1504/IJBRA.2007.015010>.
- 580 Zhang, L., Liu, C. & Davis, C.J. (2004) A mixture model-based approach to the classification of ecological
581 habitats using forest inventory and analysis data. *Canadian journal of forest research*, **34**, 1150–1156.
582 <https://doi.org/10.1139/x04-005>.
- 583 Zhou, Z.H. (2018) A brief introduction to weakly supervised learning. *National Science Review*, **5**, 44–53.
584 <https://doi.org/10.1093/nsr/nwx106>.